| | |
|---|---|
| Title | Pseudocapacitance of α-CoMoO4 nanoflakes in non-aqueous electrolyte and its bi-functional electro catalytic activity for methanol oxidation |
| Authors | Padmanathan, Narayanasamy;Shao, Han;Selladurai, Subramanian;Glynn, Colm;O'Dwyer, Colm;Razeeb, Kafil M. |
| Publication date | 2015-10-23 |
| Original Citation | Padmanathan, N., Shao, H., Selladurai, S., Glynn, C., O'Dwyer, C. and Razeeb, K. M. (2015) 'Pseudocapacitance of α-CoMoO4 nanoflakes in non-aqueous electrolyte and its bi-functional electro catalytic activity for methanol oxidation', International Journal of Hydrogen Energy, 40(46), pp. 16297-16305. doi: 10.1016/j.ijhydene.2015.09.127 |
| Type of publication | Article (peer-reviewed) |
| Link to publisher's version | http://www.sciencedirect.com/science/article/pii/S0360319915024295 - 10.1016/j.ijhydene.2015.09.127 |
| Rights | © 2015, Hydrogen Energy Publications, LLC. Published by Elsevier Ltd. All rights reserved. This manuscript version is made available under the CC-BY-NC-ND 4.0 license - http://creativecommons.org/licenses/by-nc-nd/4.0/ |
| Download date | 2024-04-10 11:59:19 |
| Item downloaded from | https://hdl.handle.net/10468/6582 |

# Pseudocapacitance of α-$CoMoO_4$ nanoflakes in non-aqueous electrolyte and its bi-functional electro catalytic activity for methanol oxidation

N. Padmanathan [a,b], Han Shao [a,c], S. Selladurai [b], Colm Glynn [c], Colm O'Dwyer [a,c], Kafil M. Razeeb [a,*]

[a] *Tyndall National Institute, Dyke Parade, Lee Maltings, Cork, Ireland*
[b] *Ionics Lab, Department of Physics, Anna University, Chennai, 25, India*
[c] *Department of Chemistry, University College Cork, Cork, Ireland*

## Abstract

Nanocrystalline cobalt molybdate ($CoMoO_4$) nanoflakes were grown directly on carbon fibre cloth (CFC) via a simple hydrothermal method without any template or surfactant. A symmetric supercapacitor was fabricated using $CoMoO_4$ nanoflakes/CFC as both negative and positive electrodes. The device has delivered the maximum specific capacitance of 8.3 F $g^{-1}$ at a constant current density of 1 A $g^{-1}$ in organic electrolyte. It offers the reasonable energy (2.6 Wh $kg^{-1}$) and power density (748.8 W $kg^{-1}$) as comparable to the carbon based symmetric supercapacitors. As a catalyst for methanol oxidation, the $CoMoO_4$ nanoflakes showed high current density (25 mA $cm^{-2}$) and low onset potential (0.38 V). The impressive bi-functional electrochemical activity of $CoMoO_4$ on CFC is mainly attributed to its porous microstructure, where reasonable electrical conductivity resulted from binder-free and intimate metal oxide/substrate integration.

## Introduction

Ever increasing energy demand and limited availability of fossil fuels coupled with high prices and environmental issues in today's globalized world are driving the search for sustainable energy storage and conversion devices [1e4]. Nevertheless, direct methanol fuel cells (DMFCs) and supercapacitors (SCs) are the most promising devices in the field of energy conversion and storage, which becomes highly desirable for various technological applications [3,5e8]. One of the most encouraging applications is their use in low-emission hybrid electric vehicles and fuel cell vehicles. In such cases, supercapacitors are coupled with fuel cells to serve as a temporary energy storage device with a high-power capability to store energies when braking [9]. Therefore, supercapacitors are likely to show equal importance to batteries and fuel cells for future energy storage systems. Similarly, the development of new catalysts (non-noble) to increase the electroactivity related to methanol oxidation is important for DMFCs [10]. It is well accepted that electrode/catalyst materials are the major component to determine

device performance, thereby they have received great attention in recent years [2,4,11e16]. In particular, non-precious and low cost transition metal oxide-based electrodes and catalysts are desirable, because they are electrochemically more active and exhibit good tolerance to surface poisoning by methanol oxidation. Therefore, recent work has been focused on the use of non-precious transition metal oxides such as NiO [17e19], $MnO_2$ [20e22], $Co_3O_4$ [23e27] and CuO [28e30] based electrode and catalyst materials for SCs as well as DMFCs. Specifically, the porous transition metal oxides are of special interest to the research community for potential applications in supercapacitors, lithium batteries and fuel cells [26]. From the earlier investigations mentioned above it is understood that the electrochemically active transition metal oxides are the most important candidates for future energy conversion/storage devices. It is also very interesting to find a material with bi-functionality (to be used in both fuel cells and supercapacitors) and enhanced electrochemical activity compared to other state of art the materials.

In recent years, metal molybdates have received considerable attention for energy storage applications in particular for supercapacitors. Among them transition metal (TM) molybdates with $ABO_4$ (A ¼ TM, B ¼ Mo) structure inclusive of $NiMoO_4$, $CoMoO_4$, $MnMoO_4$ and their hybrids have been demonstrated as the superior electrode materials for supercapacitors [31e42]. There are limited reports showing complete cell performance of these materials and in particular for non-aqueous electrolytes. Also, the methanol electrooxidation of metal molybdates have not yet been investigated. It's widely accepted that the direct integration of metal oxide nanostructures on conducting substrates can meet the practical requirements of the supercapacitor and fuel cell devices. Wei Hong et al. has constructed the $Co_3O_4$@$NiMoO_4$ hybrid nanostructure and investigated it as an asymmetric supercapacitor. Similarly, $NiCo_2O_4$ nanostructures on a conducting substrate have been reported for methanol electrooxidation by Lei Qian et al. [43]. Recently, carbon fiber cloth (CFC) has been demonstrated as an ideal flexible substrate and binder-free electrode for supercapacitors [31e33,39,40]. Unlike common metallic substrates, CFC can facilitate rapid ion/electron transport in addition to its useful characteristics for SC and DMFC applications, e.g., high conductivity (<20 mU cm), chemical stability, flexibility, and three-dimensional structures [39,42]. To date, various methods have been developed to design electrode materials onto highly flexible CFC. However, tedious and complicated synthesis processes were adopted to obtain a well-integrated 3D hierarchical architecture on flexible substrate with desired morphology. Especially for metal molybdate based electrode on CFC, only limited reports are available [35]. Recently, Di Guo et al. reported $NiMoO_4$ nanowires on CFC as the advanced electrode for symmetric supercapacitors [35]. Among the metal molybdates, $CoMoO_4$ exhibits impressive electrochemical response in both alkaline and neutral electrolytes. However, their inadequate phase in low temperature, limits their large scale applications. Therefore, it will be of great significance to develop a synthesis of $CoMoO_4$ nanostructure on a flexible substrate with desired phase and morphology.

Herein, we report a simple hydrothermal approach to design hierarchical a-$CoMoO_4$ nanoflakes on carbon fiber cloth. The electrochemical characteristic of the material has been investigated as a binder free electrode for a supercapacitor in nonaqueous electrolyte and an electrocatalyst for methanol oxidation in an alkaline medium. As an electrode for a symmetric supercapacitor, the material exhibits a maximum specific capacitance of 8.3 F $g^{-1}$ at a constant current density of 1 A $g^{-1}$ and long term cyclic stability (10,000 cycles) in 1 M Tetraethyl Ammonium Tetra Fluoroborate ($TEABF_4$) in Propylene Carbonate (PC). Interestingly, the a-$CoMoO_4$/CFC nanoflakes structure showed excellent electrocatalytic activity towards methanol oxidation with a high current density (25 mA $cm^{-2}$) and lowest onset potential (0.38 V) compared to other transition metal oxide catalysts.

## Experimental techniques

### *Fabrication*

The synthesis of a-$CoMoO_4$ nanoflakes on CFC is described as follows: CFC (4 × 4 $cm^2$), was treated with 3 M HCl for 15 min, followed by washing with ethanol and deionized water and then used as a substrate. To integrate $CoMoO_4$ on CFC, 0.1 M of $Co(NO_3)_2.6H_2O$ and 0.1 M $Na_2MoO_4.2H_2O$ were dissolved in equal volume (1:1) of water and ethanol mixed solvents separately under stirring. Molybdate ions containing solution were added drop-wise to the cobalt ion solution and stirred continuously for 30 min. A violet-colored precipitated suspension of 100 ml volume was transferred to the autoclave, which contained the pre-treated CFC substrate and was kept at 180 °C for 12 h in the oven. After that, the autoclave was left to cool to room temperature. Finally, CFC was washed with DI water and calcined for 2 h at 500 °C under Ar atmosphere. The amount of $CoMoO_4$ was measured from the weight difference of the pure CFC and $CoMoO_4$ grown CFC. The typical mass of the active electrode material is ~0.5 mg $cm^{-2}$.

### *Characterization*

The crystalline structure of the $CoMoO_4$ sample was evaluated by X-ray diffraction (Philips X'Pert Pro; Cu Ka, l ¼ 0.1542 nm). The Raman scattering spectra of $CoMoO_4$/CFC were recorded using Renishaw InVia Raman spectrometer using a 514 nm 30 mW Argon Ion laser, where spectra were collected using a RenCam CCD camera. The beam was focused onto the samples using either a 20 × /50 × objective lens. The morphology and microstructure of CFC-supported $CoMoO_4$ electrode was characterized using high resolution scanning electron microscope (HRSEM) (FEI QUANTA 200F HRSEM), and a high resolution transmission electron microscope (HRTEM) (TECNAI HRTEM-3010 at 200 kV). The capacitive performance of the samples was evaluated on a CHI 660C electrochemical workstation using cyclic voltammetry (CV), chronopotentiometry (CP), and electrochemical impedance spectroscopy (EIS) techniques. The symmetric supercapacitor was fabricated by using $CoMoO_4$/CFC as a binder-free working electrode. 1 M $TEABF_4$ in propylene carbonate (PC) solution was used as the supporting electrolyte. For fuel cell application, the electrocatalytic activity of the electrode was studied in 1 M KOH solution with and without 0.5 M $CH_3OH$ by cyclic voltammetry,

chronoamperometry and electrochemical impedance spectroscopy (EIS). A Pt wire and a saturated calomel electrode (SCE) were used as the counter and reference electrodes for this study.

## Results and discussion

### *Structure analysis*

The crystal structure of the $CoMoO_4$ grown on CFC was investigated by XRD analysis. Fig. 1(a) shows the XRD pattern of $CoMoO_4$ nanoflakes and the inset represents the XRD pattern of pure CFC. The broad peak with splitting at ~26.10° can be assigned to the (002) plane of a-$CoMoO_4$ as well as the reflection of CFC [41]. Similarly, the diffraction peaks positioned at 27.4°, 31.2°, 34.1°, 37.08°, 39°, 42.6° and 47.1° can be indexed to the (-112), (131), (-222), (040), (003), (132) and (-511) planes of a-$CoMoO_4$. The observed broad diffraction peaks can be ascribed to the formation of nanocrystalline a-$CoMoO_4$ which is well-matched to the corresponding JCPDS file (21e0868) [31,44]. In order to avoid the confusion of crystalline structure, the XRD analysis of the powder sample collected from the remaining precipitate formed during the hydrothermal process was carried out and is shown in Fig. S1. It further supports the formation of a-$CoMoO_4$ nanocrystalline. Raman scattering analysis further confirmed the formation of $CoMoO_4$ on carbon fibre cloth. Fig. 1(b) shows the Raman spectra of $CoMoO_4$ nanoflakes on CFC and the inset represents the Raman bands of pure CFC. The observed Raman bands for $CoMoO_4$ are 333, 363, 697, 808, 884 and 928 $cm^{-1}$. The bands at 884 and 928 $cm^{-1}$ and the low wavenumber band at 333 $cm^{-1}$ are related to the Mo-Oe-Co stretching vibrations in $CoMoO_4$ [44,45]. The Co-O vibrational band was observed at 528 $cm^{-1}$ [45]. The band at 697 $cm^{-1}$ further confirms the formation of a-$CoMoO_4$, which is in good agreement with XRD results [46]. As with pure CFC, the high intensity D band (disordered carbon) and G band (graphitic carbon) of carbon are found with Raman shifts of ~1353 and 1581 $cm^{-1}$, respectively (see inset of Fig. 1(b)) [47].

The surface morphology of $CoMoO_4$ directly grown on CFC was examined by SEM and TEM. Fig. 2(a-d) shows the SEM images of $CoMoO_4$ on CFC. The low magnification SEM images as shown in Fig. 2(a and b) showed the growth of well-integrated nanoflakes over the CFC surface in a uniform manner. The $CoMoO_4$ completely covered the CFC with interconnected nanoflakes. The high magnification SEM images of Fig. 2(d) clearly shows that the nanoflakes are composed of fine nanocrystals and exhibit an open network of porous microstructure. It should be noted that this interesting microstructure can provide large volume space to accommodate electrolyte ions and increase active sites to the redox process. The composition of the elements present in $CoMoO_4$ nanoflakes are confirmed with energy dispersive X-ray spectrum (EDS) analysis, which is shown in Fig. S2 (ESI). The EDS shows the dominant carbon peak from the substrate in addition to the primary Co, Mo and O elements in appropriate concentrations. This result confirms the phase purity of the compound. Typical TEM images of Fig. 3(a) and (b) indicate the nanocrystals of 7e12 nm randomly oriented, and form the interconnected nanoflake microstructure. From high magnification TEM images of Fig. 3(c), the characteristic porous microstructures of $CoMoO_4$ nanoflakes are visible. The selected area electron diffraction pattern (SAED) shown in Fig. 3(d) confirms the polycrystalline growth of a-$CoMoO_4$ over the CFC. The selected rings are well matched to the corresponding {*hkl*} planes of standard $CoMoO_4$ nanocrystals. Based on this observation, the growth of $CoMoO_4$ nanoflakes can be described by the following chemical reactions [48]:

$$Co^{2+} + MoO_4^{2-} + \frac{H_2O}{C_2H_5OH} \rightarrow [Co^{2+}MoO_4^{2-}(H_2O)] \quad (1)$$

$$[Co^{2+}MoO_4^{2-}(H_2O)] \xrightarrow{500\ ^\circ C\ in\ Ar\ (2h)} CoMoO_4 \quad (2)$$

Initially, hydrated cobalt molydate complex was formed, which may interact electrostatically with the CFC. Under hydrothermal conditions, nucleation of $CoMoO_4$ occurred, followed by the growth of $CoMoO_4$ nanoflakes on the CFC surface.

### *Symmetric supercapacitor*

The electrochemical characteristic of the $CoMoO_4$ nanoflakes electrodes was investigated as a symmetric supercapacitor in 1 M $TEABF_4$ in PC electrolyte by cyclic voltammetry, charge-discharge and electrochemical impedance measurements. Typical electrochemical responses of $CoMoO_4$/CFC are shown in Fig. 4(a-d). Cyclic voltammograms of

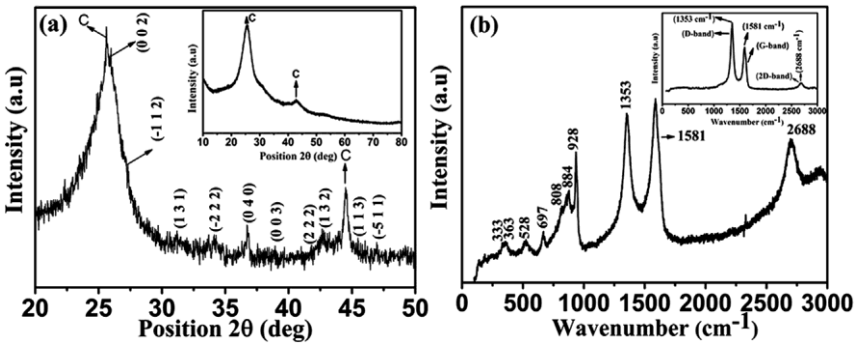


Fig. 1 (a) XRD pattern and (b) Raman spectrum of $CoMoO_4$/CFC and pristine CFC.

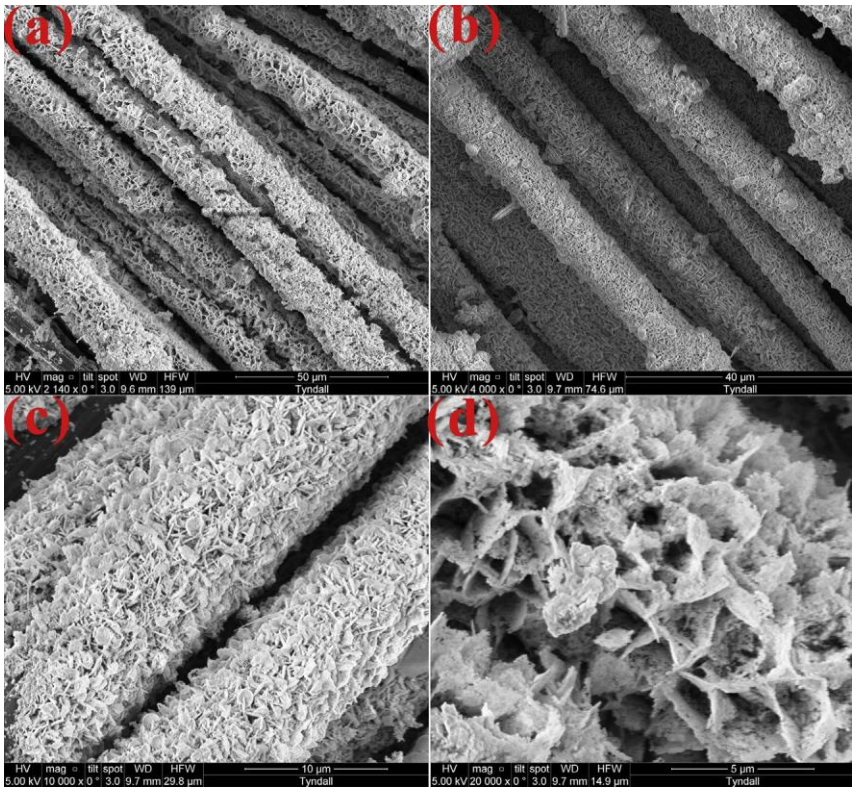


Fig. 2 (a-d) HRSEM images of $CoMoO_4$ nanoflakes structure on CFC.

$CoMoO_4||CoMoO_4$ supercapacitor in various voltage windows at a scan rate of 100 $mV^{-1}$ is shown in Fig. S3(a). It can be seen that the $CoMoO_4$ electrode has good electrochemical activity in a broad potential window in 1 M $TEABF_4$/PC electrolyte. For a potential range of -1 to 1.5 V, the CV curve exhibits characteristic rectangular shape and indicates an ideal capacitive behaviour. As the potential increases to 2.5 V, the shape of the CV curve deviates from their rectangular shape due to the

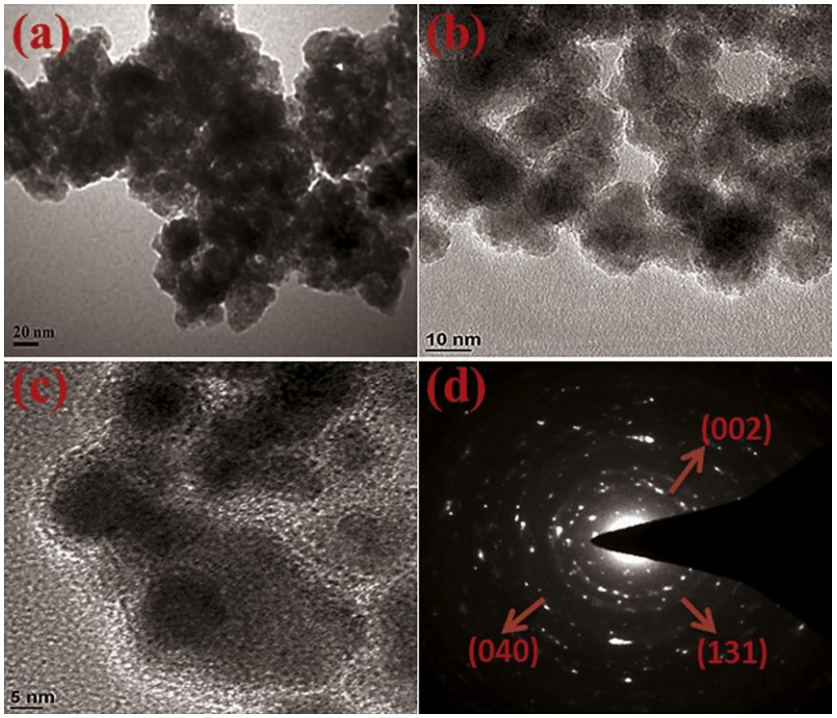


Fig. 3 (a-c) HRTEM images of $CoMoO_4$ nanoflakes, (d) the corresponding SAED pattern.

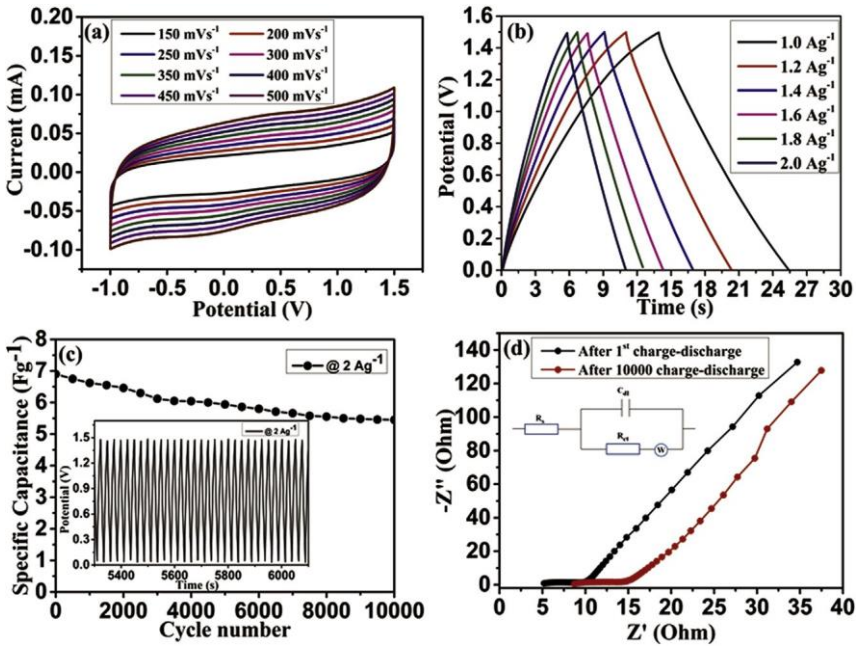


Fig. 4 (a) Cyclic voltammogram of $CoMoO_4$/CFC symmetric supercapacitor at various scan rates in 1 M $TEABF_4$/PC (b) Charge/discharge curves of symmetric supercapacitor at different current densities, (c) Cyclic stability at 2 A $g^{i1}$ over 10000 cycles (d) Nyquist plot of symmetric supercapacitor in 1 M $TEABF_4$/PC.

electrolyte decomposition. To date, the scan rate reported for metal oxide-based symmetric supercapacitors is limited to 200 mV $s^{-1}$ [35]. However, for practical applications this rate capability is not sufficiently high to provide higher energy and needs to be improved. In this study, we have measured the CV at different scan rates, ranging from 100 to 12,000 mV $s^{-1}$ and are depicted in Fig. 4(a) and Fig. S3(bed). From Fig. 4(a), it indicates that the supercapacitor maintained its rectangular shape and reversibility even at the high scan rate of 500 mV $s^{-1}$.

When the scan rate increased from 600 to 5000 mV $s^{-1}$, our symmetric supercapacitor retained the voltammetric shape and featureless current response at both anodic and cathodic sweeps as shown in Fig. S3(c and d), which demonstrate the ultra-fast rate capability of the device. At very high scan rates ranging from 6000 to 12000 mV $s^{-1}$, the device responds with rectangular CV features with slight deviation at the end potentials. This result further confirms the high-rate performance of the device. The specific capacitances with respect to scan rates are shown in Fig. S4 and the values are presented in Table 1 of ESI. The galvanostatic charge-discharge profiles measured in positive potential at different current densities is shown in Fig. 4(b) and reveals nearly linear time-potential relation, which describes the capacitive characteristic of the material. The specific capacitance ($C_s$) of the electrode was determined using the following equation:

$$C_s = I\Delta t = m\Delta V \quad (3)$$

where, $I$ is the charge/discharge current, $t$ is discharge time, D$V$ is the potential limit during discharge, and $m$ is the mass of the active material. While calculating the specific capacitance for $CoMoO_4$/CFC, the contribution of CFC was subtracted from the total $C_s$ value. To convince us of the contribution of CFC on specific capacitance we have measured the CV and char- ge-discharge for pure CFC in two electrode configuration with the same electrolyte. Fig. S5(a and b) shows the CV and charge-discharge curves of pristine CFC based symmetric supercapacitor. The CV curve at different scan rates ranging from 20 to 1000 $mV^{-1}$ showed the capacitive characteristic of the CFC. However, the observed current response is 1000 times lower than the $CoMoO_4$/CFC based supercapacitor, which describes a negligible contribution by the CFC to the measured capacitance. Similarly, the charge-discharge profile also clearly evidences the ideal capacitive behaviour with insignificant discharge time (only few seconds) as shown in Fig. S5(b) and delivered the specific capacitance of ~1 mF $cm^{-2}$ @ 0.5 mA $cm^{-2}$. Therefore it can be concluded that the measured capacitance mainly arises from the $CoMoO_4$ nanoflakes and not from the CFC.

The specific capacitances for $CoMoO_4$/CFC based supercapacitor are found to be 8.3, 7.3, and 6.9 F $g^{-1}$ for the corresponding current densities of 1, 1.4 and 2 $Ag^{-1}$, respectively. 83% of initial capacitance was retained when the current density was increased to ~2 A $g^{-1}$, which indicates the very good capacity retention of the supercapacitor. This result was further compared with 3 M KOH electrolyte. Typical CV and charge/discharge curves of the $CoMoO_4$/CFC based symmetric supercapacitor measured in 3 M KOH electrolyte are shown Fig. S6(a and b). From the CV curves, the pseudo-capacitive characteristic of the device over the scan rates ranging from 10 to 100 mV $s^{-1}$ can be observed. The charge-discharge profiles also are in concordance with the CV results. The measured specific capacitances in 3 M KOH electrolytes are found to be 25.2, 16.9 and 9.3 F $g^{-1}$ for a current density of 0.5,

1.5 and 2.5 A $g^{-1}$, respectively. The observed specific capacitance in organic electrolyte is comparatively lower than the metal molybdate based symmetric supercapacitors investigated in alkaline electrolytes [35]. This may be due to the limited number of larger size organic (~1.4 nm) electrolyte ion diffusion via the inhomogeneous electrode pores and lead to partial contribution of surface active sites to the redox process [49,50]. In order to increase the capacitance value further, investigation is required on this material with a different electrolyte system. To date, aqueous electrolytes (KOH, $H_2SO_4$, etc.) are widely used to investigate the electrochemical capacitive features of the porous electrodes due to their high ionic conductivity and smaller ionic (~0.5 nm) size. However, their narrow potential window (~1 V), electrolyte leakage, corrosive behaviour and lower energy and power density, limits their large scale practical applications. Therefore, it is important to investigate the pseudo-electrochemical performance of the metal oxide electrodes in organic electrolyte systems. In organic electrolytes, it is possible to further extend the potential window to ~2.5 V, thereby enhancing the energy and power densities of the supercapacitor devices. Also, negligible leakage and limited corrosion by the organic electrolyte over long term usage, further increase the life span of the supercapacitors. However, the average specific capacitance in organic electrolytes is still quite low as compared to inorganic electrolytes and needs to be improved.

The long term cyclic stability of the symmetric supercapacitor was tested by continuous charge-discharge measurement over 10,000 cycles at a constant current density of 2 A $g^{-1}$ Fig. 4(c) shows the cyclic performance of the $CoMoO_4||CoMoO_4$ supercapacitor in organic electrolyte. The response confirms that the device exhibits an excellent cyclic stability and delivered 78.9% of capacitance retention after 10,000 cycles. To further understand the electrochemical kinetics electrochemical impedance analysis was carried out before and after 10,000 charge-discharge cycles. A typical Nyquist plot is shown in Fig. 4(d) together with the corresponding equivalent circuit. According to the equivalent cir- cuit, $R_s$, $C_{dl}$, $R_{ct}$, and $W$ are the solution resistance, double layer capacitance, charge transfer resistance and Warberg's diffusion elements, respectively [47,51]. The device displays a pure capacitive behavior at low frequency and significant charge transfer kinetics at high frequencies. The estimated charge transfer resistance is 5.95 U and it was slightly increased to 6.14 U after 10,000 charge-discharge cycles. This result further supports the good electrical conductivity of the materials and low contact resistance at the electrode/electrolyte interfaces. The power and energy performance of the device was calculated using the following relations:

$$E = CV^2/2 \quad (4)$$

$$P = E/t \quad (5)$$

where $E$ is the energy density, $C$ is the specific capacitance, $V$ is the potential limit, P is power density and $t$ is discharge time. The active mass based energy and power density relation for $CoMoO_4||CoMoO_4$ symmetric supercapacitor is shown Fig. 5. Our device delivered an energy density of 2.6 Wh $kg^{-1}$ with the

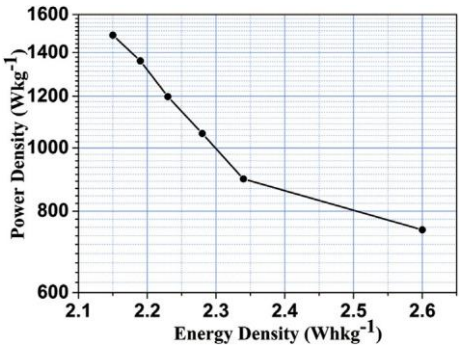


Fig. 5 Ragone plot of $CoMoO_4$/CFC based symmetric supercapacitor in 1 M $TEABF_4$.

power outcome of 748.8 W $kg^{-1}$ at a current density of 1 $Ag^{-1}$. When the current density was increased to 2 $Ag^{-1}$, the device exhibited 2.2 Wh $kg^{-1}$ of energy with 1488.5 W $kg^{-1}$ of power density. The observed energy and power performance of the organic electrolyte based symmetric supercapacitor is considerably higher than the symmetric supercapacitor measured in 3 M KOH. The inorganic device has delivered a specific energy density of only 2 Wh $kg^{-1}$ with a power density of 400 W $kg^{-1}$ at the same current density of 1 $Ag^{-1}$. Further increasing the current density to 2 A $g^{-1}$, the energy and power density decreased to 0.9 Wh $kg^{-1}$ and 800 W $kg^{-1}$, respectively. This increased energy and power performance of organic supercapacitor is mainly due to the increased potential window. However, only few reports are available where metal oxide based symmetric cell performance is investigated, particularly in the organic electrolytes [27,52]. In comparison to our earlier investigations, the present work with $CoMoO_4$/CFC electrode has delivered significant energy and power performance as comparable to the different metal oxide electrodes measured in inorganic electrolyte systems. Interestingly, the materials showed good capacitive behaviour in 1 M $TEABF_4$ with excellent rate capability up to 12000 mV $s^{-1}$ and reasonable specific capacitance. Also, our device exhibits superior cyclic stability with 78.9% capacity retention even after 10,000 cycles. These results show an improvement over devices from Veerasubramani et al., where they showed 84.7% retention after 4000 cycles at a current density of 1 mA $cm^{-2}$ in 1 M NaOH [53]. Our specific capacitance is significantly higher than the value reported for a hydrogenated ZnO core-shell nanocable based flexible supercapacitor (26 mF $cm^{-2}$ @ 0.5 $mAcm^{-2}$) [54] and an Ru//Ru symmetric supercapacitor in 1 M $Na_2SO_4$ aqueous electrolyte, which showed only 67 mF $cm^{-2}$ @ 1 mA $cm^{-2}$ [55]. Also, this value is much higher than the symmetric capacitor based on $Co_3O_4$ nanowire/nanoflower/CFC hybrid structure in both 1 M $TEABF_4$ (4.8 mF $cm^{-2}$ @ 3 mA $cm^{-2}$) and 3 M KOH (7.8 mF $cm^{-2}$) electrolytes [27]. It should be noted that the energy and power performance of the $CoMoO_4$ based supercapacitor in organic electrolytes compares favourably with carbon-based symmetric devices [51]. Thereby, $CoMoO_4$ on CFC with a functional morphology and pore distribution is a potential electrode for supercapacitor application.

*Electro-oxidation of methanol*

The electrocatalytic activity of $CoMoO_4$ nanoflakes towards methanol oxidation in alkaline medium was studied by cyclic voltammetry and chronoamperometry analysis. Typical catalytic response of $CoMoO_4$ catalyst in 1 M KOH þ0.5 M $CH_3OH$ is shown in Fig. 6(a-d). The CV curves in Fig. 6(a) indicate an excellent electroϵcatalytic activity of $CoMoO_4$ electrode by showing the well resolved redox peaks without methanol (Black) and effective methanol oxidation with high current density in the presence of methanol (Red). The electrode showed a peak current density of 25 mA $cm^{-2}$ at 0.7 V. More importantly, our $CoMoO_4$/CFC electrode exhibits a low onset potential of 0.38 V, lower than NiO (0.5 V), $NiCo_2O_4$ (0.42 V) and $Co_3O_4$ (0.56 V) catalysts grown on conducting substrates [43]. Thereby, it may be concluded that the $CoMoO_4$/CFC has excellent electrocatalytic activity towards methanol oxidation. It can be noticed in Fig. 6(b) that increasing the scan rate from 5 to 50 mV $s^{-1}$ resulted in the increase in oxidation current without any deviation in the redox peaks, even at the high scan rate of 50 mV $s^{-1}$. This result indicates the rapid electron/ion transfer kinetics in the electrode surface during methanol oxidation that is not limited by diffusion. The stability of the catalyst is one of the important factors for the usability of the electrode for longer time. Thereby, it was investigated with a chronoamperometric curve recorded for an extended time of 3000 s at an initial voltage of 0.38 V. As from Fig. 6(c), it can be seen that the electrode showed a sudden decay for a few seconds followed by stable current for 3000 s, which inferred the excellent electrochemical stability of the catalyst. The catalyst showed a high current density even after 3000 s. This result confirmed that the $CoMoO_4$ nanoflake structure has a better tolerance towards the tenacious reaction intermediates such as CO and HCHO, which are usually formed during methanol oxidation to contribute to electrode poisoning [43].

Fig. 6(d) presents the Nyquist plots for $CoMoO_4$/CFC recorded in 1 M KOH and 0.5 M $CH_3OH$ in 1 M KOH. The measured impedance spectra showed a sloped line at low frequencies, relating to the diffusion process and semicircle at high frequency region due to electron transfer [56]. The observed incomplete semicircle infers the frequency limitation of the measurement. It is noticeable that the diameter of the semicircle is small, which is due to the superior electrical conductivity of the catalyst in 0.5 M $CH_3OH$. The observed impedance spectra were compared to the equivalent circuit as given in the inset of Fig. 6(d). From Fig. 6(d), the measured $R_{ct}$ value is small (~3.72 Ω) for methanol electro-oxidation in 1 M KOH, indicating good tolerance of the catalyst against CO poisoning. Furthermore, it confirmed the effective contribution of $Co^{2+}/Co^{3+}$ for the methanol oxidation process, which resulted in a high catalytic current density. Thereby, it validated the usability of the $CoMoO_4$ nanoflakes on carbon fiber cloth as a potential electro-catalyst for methanol oxidation reaction.

The interesting bi-functional electrochemical features of hydrothermally grown $CoMoO_4$ nanoflake/CFC electrode were possibly due to their desired structural benefits. In brief, the highly flexible and conducting carbon fiber cloth substrate provided the good mechanical integrity and adhesion

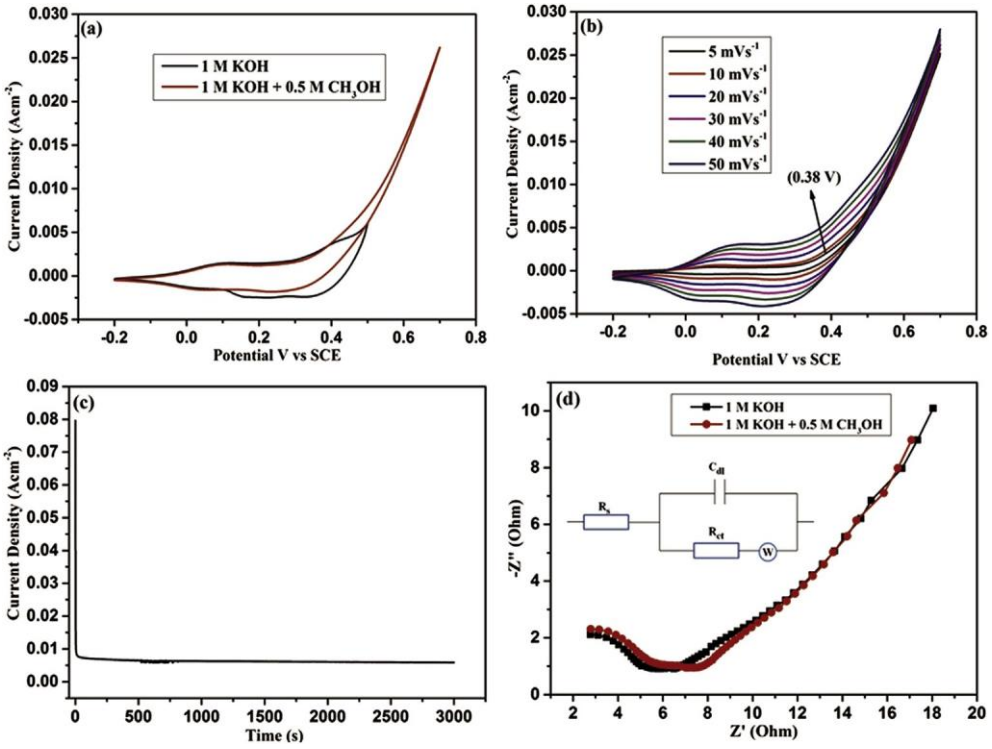


Fig. 6 (a) Cyclic voltammogram of $CoMoO_4$/CFC measured in 1 M KOH and 1 M KOH +0.5 M $CH_3OH$ at 20 mV $s^{-1}$ (b) CV curves of methanol oxidation with various scan rates. (c) Amperometric curve of $CoMoO_4$/CFC hybrid electrode and (d) Nyquist plot for $CoMoO_4$ catalyst with and without methanol.

between electroactive material and substrate area during faradaic reaction. Consequently, the nanoflakes have offered high exposed surface to electrolyte contact, which significantly enhanced the core-level redox process. The direct contact between metal oxide and CFC further supported the high electrical conductivity. Overall from this investigation it can be inferred that the growth of $CoMoO_4$ nanostructure on CFC can be used as a bi-functional electrode for both supercapacitor as well as direct methanol fuel cell applications.

## Conclusions

In summary, porous $CoMoO_4$ nanoflakes consisting of ultrafine nanocrystals were grown directly on the carbon fiber cloth by hydrothermal approach and were demonstrated to be superior bi-functional electrode material for energy storage and conversion devices. As a binder free electrode for symmetric supercapacitor, the $CoMoO_4$/CFC exhibited good electrochemical performance in 1 M $TEABF_4$ non-aqueous electrolyte with reasonable specific capacitance of 8.3 $Fg^{-1}$ at a constant current density of 1 $Ag^{-1}$. Furthermore, the capacitor showed reasonable energy and power performances and also showed good electrochemical reversibility for long term applications. Interestingly, the $CoMoO_4$/CFC showed methanol electro-oxidation with high current density (25 mA $cm^{-2}$) at lowest onset potential (0.38 V) as an anode material for DMFC. This bi-functional electrochemical activity of the electrode is mainly due to the advantages through their desired 3D hierarchical porous nanoflake microstructure, good electrical conductivity, and integration of $CoMoO_4$ with CFC.

## Acknowledgements

The authors acknowledge the financial support from EU FP7 project MANpower (contract number: 604360) to carry out this work. C.G. acknowledges the support of the Irish Research Council under awards RS/2011/797. This work was also supported by SFI under the National Access Programme (NAP 417).

## Appendix A. Supplementary data

Supplementary data related to this article can be found at http://dx.doi.org/10.1016/j.ijhydene.2015.09.127.

## References

[1] Winter M, Brodd RJ. What are batteries, fuel cells, and supercapacitors? Chem Rev 2004;104:4245e69.
[2] Arico AS, Bruce P, Crosati B, Tarascon J, Schalkwijk WV. Nanostructured materials for advanced energy conversion and storage devices. Nat Mater 2005;4:366e77.
[3] Miller JR, Simon P. Electrochemical capacitors for energy management. Science 2008;321:651e2.
[4] Simon P, Gogotsi Y. Materials for electrochemical capacitors. Nat Mater 2008;7:845e54.
[5] Kamarudin SK, Daud WRW, Ho SL, Hasran UA. Overview on the challenges and developments of micro-direct methanol fuel cells (DMFC). J Power Sources 2007;163:743e54.
[6] Meng F, Ding Y. Sub-micrometer-thick all-solid-state supercapacitors with high power and energy densities. Adv Mater 2011;23:4098e102.
[7] Tan YB, Lee J-M. Graphene for supercapacitor applications. J Mater Chem A 2013;1:14814.
[8] Ren X, Zelenay P, Thomas S, Davey J, Gottesfeld S. Recent advances in direct methanol fuel cells at Los Alamos National Laboratory. J Power Sources 2000;86:111e6.
[9] Zhang LL, Zhao XS. Carbon-based materials as supercapacitor electrodes. Chem Soc Rev 2009;38:2520e31.
[10] Franco EG, Oliveira-Neto A, Spinace EV, Linardi M, Martz N, Mazurek M, et al. Synthesis and characterization of PtRu/C catalysts obtained by colloidal and deposition methods for fuel cell applications. Mater Res 2005;8:117e20.
[11] Wachs IE. Recent conceptual advances in the catalysis science of mixed metal oxide catalytic materials. Catal Today 2005;100:79e94.
[12] Zhao X, Sanchez BM, Dobson PJ, Grant PS. The role of nanomaterials in redox-based supercapacitors for next generation energy storage devices. Nanoscale 2011;3:839e55.
[13] Wang G, Zhang L, Zhang J. A review of electrode materials for electrochemical supercapacitors. Chem Soc Rev 2012;41:797e828.
[14] Zhi M, Xiang C, Li J, Li M, Wu N. Nanostructured carbon-metal oxide composite electrodes for supercapacitors: a review. Nanoscale 2013;5:72e88.
[15] Huang H, Wang X. Recent progress on carbon-based support materials for electrocatalysts of direct methanol fuel cells. J Mater Chem A 2014;2:6266.
[16] Cameron DS, Hards GA, Harrison B, Potter RJ. Direct methanol fuel cells. Platin Met Rev 1987;31:173e81.
[17] Barakat NA, Abdelkareem MA, El-Newehy M, Kim HY. Influence of the nanofibrous morphology on the catalytic activity of NiO nanostructures: an effective impact toward methanol electrooxidation. Nanoscale Res Lett 2013;8:402.
[18] Han D, Xu P, Jing X, Wang J, Yang P, Shen Q, et al. Trisodium citrate assisted synthesis of hierarchical NiO nanospheres with improved supercapacitor performance. J Power Sources 2013;235:45e53.
[19] Elzatahry A. Polyacrylonitril electrospun nanofiber as a template to prepare NiO nanostructure electrocatalyst. Int J Electrochem Sci 2014;9:22e31.
[20] Nam K-W, Lee C-W, Yang X-Q, Cho BW, Yoon W-S, Kim K-B. Electrodeposited manganese oxides on three-dimensional carbon nanotube substrate: supercapacitive behaviour in aqueous and organic electrolytes. J Power Sources 2009;188:323e31.
[21] Cheng F, Su Y, Liang J, Tao Z, Chen J. $MnO_2$-based nanostructures as catalysts for electrochemical oxygen reduction in alkaline mediay. Chem Mater 2010;22:898e905.
[22] Fan Z, Yan J, Wei T, Zhi L, Ning G, Li T, et al. Asymmetric supercapacitors based on graphene/$MnO_2$ and activated carbon nanofiber electrodes with high power and energy density. Adv Funct Mater 2011;21:2366e75.
[23] Al-Enizi AM, Elzatahry AA, Soliman AI, Al-Theyab SS. Electrospinning synthesis and electrocatalytic performance of cobalt oxide/carbon nanofibers nanocomposite based PVA for fuel cell applications. Int J Electrochem Sci 2012;7:12646e55.
[24] Yang L, Cheng S, Ding Y, Zhu X, Wang ZL, Liu M. Hierarchical network architectures of carbon fiber paper supported cobalt oxide nanonet for high-capacity pseudocapacitors. Nano Lett 2012;12:321e5.

[25] Deori K, Ujjain SK, Sharma RK, Deka S. Morphology controlled synthesis of nanoporous $Co_3O_4$ nanostructures and their charge storage characteristics in supercapacitors. ACS Appl Mater Interfaces 2013;5:10665e72.
[26] Roy M, Ghosh S, Naskar MK. Synthesis of morphology controllable porous $Co_3O_4$ nanostructures with tunable textural properties and their catalytic application. Dalton Trans 2014;43:10248e57.
[27] Padmanathan N, Selladurai S, Razeeb KM. Ultra-fast rate capability of a symmetric supercapacitor with a hierarchical $Co_3O_4$ nanowire/nanoflower hybrid structure in non-aqueous electrolyte. RSC Adv 2015;5:12700e9.
[28] Wang G, Huang J, Chen S, Gao Y, Cao D. Preparation and supercapacitance of CuO nanosheet arrays grown on nickel foam. J Power Sources 2011;196:5756e60.
[29] Qiu G, Dharmarathna S, Zhang Y, Opembe N, Huang H, Suib SL. Facile microwave-assisted hydrothermal synthesis of CuO nanomaterials and their catalytic and electrochemical properties. J Phys Chem C 2012;116:468e77.
[30] Zhang X, Shi W, Zhu J, Kharistal DJ, Zhao W, Lalia BS, et al. High-power and high-energy-density flexible pseudocapacitor electrodes made from porous CuO nanobelts and single-walled carbon nanotubes. ACS Nano 2011;5:2013e9.
[31] Guo D, Zhang H, Yu X, Zhang M, Zhang P, Li Q, et al. Facile synthesis and excellent electrochemical properties of $CoMoO_4$ nanoplate arrays as supercapacitors. J Mater Chem A 2013;1:7247.
[32] Senthilkumar B, Meyrick D, Lee Y-S, Selvan RK. Synthesis and improved electrochemical performances of nano b-$NiMoO_4$e$CoMoO_4$\$x$H_2O$ composites for asymmetric supercapacitors. RSC Adv 2013;3:16542.
[33] Xia X, Lei W, Hao Q, Wang W, Wang X. One-step synthesis of $CoMoO_4$/graphene composites with enhanced electrochemical properties for supercapacitors. Electrochimica Acta 2013;99:253e61.
[34] Cai D, Liu B, Wang D, Liu Y, Wang L, Li H, et al. Enhanced performance of supercapacitors with ultrathin mesoporous $NiMoO_4$ nanosheets. Electrochimica Acta 2014;125:294e301.
[35] Guo D, Luo Y, Yu X, Li Q, Wang T. High performance $NiMoO_4$ nanowires supported on carbon cloth as advanced electrodes for symmetric supercapacitors. Nano Energy 2014;8:174e82.
[36] Ma X-J, Kong L-B, Zhang W-B, Liu M-C, Luo Y-C, Kang L. Facile fabrication and perfect cycle stability of 3D NiO@$CoMoO_4$ nanocomposite on Ni foam for supercapacitors. RSC Adv 2014;4:17884.
[37] Ma X-J, Kong L-B, Zhang W-B, Liu M-C, Luo Y-C, Kang L. Design and synthesis of 3D $Co_3O_4$@$MMoO_4$ (M¼Ni, Co) nanocomposites as high-performance supercapacitor electrodes. Electrochimica Acta 2014;130:660e9.
[38] Padmanathan N, Razeeb KM, Selladurai S. Hydrothermal synthesis of carbon- and reduced graphene oxide-supported $CoMoO_4$ nanorods for supercapacitor. Ionics 2014;20:1323e34.
[39] Veerasubramani GK, Krishnamoorthy K, Radhakrishnan S, Kim N-J, Kim SJ. Synthesis, characterization, and electrochemical properties of $CoMoO_4$ nanostructures. Int J Hydrogen Energy 2014;39:5186e93.
[40] Moosavifard SE, Shamsi J, Ayazpour M. 2D high-ordered nanoporous $NiMoO_4$ for high-performance supercapacitors. Ceram Int 2015;41:1831e7.
[41] Xu Z, Li Z, Tan X, Holt CMB, Zhang L, Amirkhiz BS, et al. Supercapacitive carbon nanotube-cobalt molybdate nanocomposites prepared via solvent-free microwave synthesis. RSC Adv 2012;2:2753e5.
[42] Lin Y, Pang H, Guo J, Wang W, Yan Z, Ma L, et al. Hydrated cobalt nickel molybdate nanorods as effectively supercapacitor electrode materials. Int J Electrochem Sci 2013;8:2945e57.
[43] Qian L, Gu L, Yang L, Yuan H, Xiao D. Direct growth of $NiCo_2O_4$ nanostructures on conductive substrates with enhanced electrocatalytic activity and stability for methanol oxidation. Nanoscale 2013;5:7388e96.
[44] Cherian CT, Reddy MV, Haur SC, Chowdari BV. Interconnected network of CoMoO(4) submicrometer particles as high capacity anode material for lithium ion batteries. ACS Appl Mater Interfaces 2013;5:918e23.
[45] Herrera JE, Resasco DE. Role of Co-W interaction in the selective growth of single-walled carbon nanotubes from CO disproportionation. J Phys Chem 2003;107:3738e46.
[46] APd Moura. Photoluminescent properties of $CoMoO_4$ nanorods quickly synthesized and annealed in a domestic microwave oven. Adv Chem Eng Sci 2012;02:465e73.
[47] Padmanathan N, Selladurai S. Controlled growth of spinel $NiCo_2O_4$ nanostructures on carbon cloth as a superior electrode for supercapacitors. RSC Adv 2014;4:8341.
[48] Xiao W, Chen JS, Li CM, Xu R, Lou XW. Synthesis, characterization, and lithium storage capability of $AMoO_4$(A ¼ Ni, Co) nanorods. Chem Mater 2010;22:746e54.
[49] Gao W, Singh N, Song L, Liu Z, Reddy AL, Ci L, et al. Direct laser writing of micro-supercapacitors on hydrated graphite oxide films. Nat Nanotechnol 2011;6:496e500.
[50] Yang CM, Kin YJ, Endo M, Kanoh H, Yudasaka M, Lijima S, et al. Nanowindow-regulated specific capacitance of supercapacitor electrodes of single-wall carbon nanohorns. J Am Chem Soc 2007;129:20e1.
[51] Vilian ATE, Rajkumar M, Chen S-M, Hu C-C, Boopathi KM, Chu C-W. High electrocatalytic performance of platinum and manganese dioxide nanoparticle decorated reduced graphene oxide sheets for methanol electro-oxidation. RSC Adv 2014;4:41387e97.
[52] Padmanathan N, Selladurai S, Mani Rahulan K, O'Dwyer Colm, Razeeb KM. NiO hybrid nanoarchitecture-based pseudocapacitor in organic electrolyte with high rate capability and cycle life. Ionics 2015;21(9):2623e31.
[53] Veerasubramani GK, Krishnamoorthy K, Kim SJ. Electrochemical performance of an asymmetric supercapacitor based on graphene and cobalt molybdate electrodes. RSC Adv 2015;5:16319e27.
[54] Yang P, Xiao X, Li Y, Ding Y, Qiang P, Tan X, et al. Hydrogenated ZnO coreshell nanocables for flexible supercapacitors and self-powered systems. ACS Nano 2013;7:2617e26.
[55] Xia H, Li B, Lu L. 1.8 V symmetric supercapacitors developed using nanocrystalline Ru films as electrodes. RSC Adv 2014;4:11111.
[56] Zhu Y, Murali S, Stoller MD, Ganesh KJ, Cai W, Ferreira PJ, et al. Carbon-based supercapacitors produced by activation of graphene. Science 2011;332:1537e41.